# The Initial Post-buckling Behavior of Face-Sheet Delaminations in Sandwich Composites

**G. A. Kardomateas**
Professor,
Fellow ASME

**H. Huang**[1]
Post-doctoral Fellow

School of Aerospace Engineering,
Georgia Institute of Technology,
Atlanta, GA 30332-0150

*Should an interface crack between the layers of the composite face-sheet or between the core and the composite face-sheet of a sandwich beam/plate exists, local buckling and possible subsequent growth of this interface crack (delamination) may occur under compression. In this study, the buckling, and initial post-buckling behavior is studied through a perturbation procedure that is based on the nonlinear beam equations with transverse shear included. Closed-form solutions for the load and midpoint delamination deflection versus applied compressive strain during the initial postbuckling phase are derived. Illustrative results are presented for several sandwich construction configurations, in particular with regard to the effect of material system and transverse shear.*
[DOI: 10.1115/1.1532320]

## Introduction

Delaminations (layer interface cracks) constitute a common failure phenomenon in laminated composites and they are most easily introduced from impact loads. These delaminations may deteriorate the performance of the structure under compressive loading (e.g., Yin et al. [1] and Simitses et al. [2]). A large number of studies on the behavior of delamination buckling and post-buckling in composites have been carried out by many researchers, e.g., Chai et al. [3] by using a one-dimensional model, Whitcomb [4] and Shivakumar and Whitcomb [5] by using finite elements and Rayleigh-Ritz analysis, Kardomateas [6] by conducting monotonic compressive tests, Kardomateas [7] by using elastica theory to account for large deformations during post-buckling, Kardomateas et al. [8] by studying both experimentally and analytically the fatigue growth of delaminations during cyclic compression, etc.

Although the general principles are not very different, delamination failure in sandwich structures is just beginning to be explored in detail. In this regard, differences in the behavior of delamination buckling and post-buckling within a sandwich structure from that of a laminated composite structure arise due to the fact that the substrate in a delaminated sandwich structure includes a much different kind of material, namely a transversely flexible core made of foam or low strength honeycomb. To this extent, the contribution of the shear stresses and shear deformations of the core are expected to be noteworthy and therefore should be included in the formulation.

A typical sandwich structure is composed of two thin composite laminated faces and a thick soft core made of foam or low strength honeycomb. Due to its exceptional properties, mainly high stiffness and strength with little resultant weight penalty, sandwich structures have been used in aircraft, marine, and other types of structures. Research into sandwich structural behavior and failure modes can be traced following World War II in a rather sporadic fashion but intensified in the 1990s, especially with regard to proper modeling of the core through high-order theories (e.g., Kant and Patil [9], Hunt and Da Silva [10,11], Frostig [12], and Frostig and Baruch [13]). Recently, there have been many contributions presented at symposia dedicated to sandwich structures, e.g. Rajapakse et al. [14].

Although these high-order theories are expected to render most accurate results, they involve considerable effort in addressing the complexities of the formulation of the problem of post-buckling of delaminated beams, and therefore, in the present work, a nonlinear beam equation including transverse shear, properly formulated for an unsymmetric sandwich section (meaning face sheets not of the same geometry and/or material) is used to model the delaminated, substrate, and base parts. The same approach can be used to study either a delamination within the face sheet or a debond at the interface between the face sheet and the core.

## Formulation

**Governing Equations and Boundary Conditions.** Let us consider a sandwich beam, of length $2L$, and width $w$, consisting of two face sheets of thickness $f_1$ and $f_2$, extensional moduli $E_{f1}$ and $E_{f2}$, and shear moduli $G_{f1}$ and $G_{f2}$, respectively. The core, of thickness $c$, has an extensional modulus, $E_c$, and shear modulus $G_c$ (Fig. 1). The delamination, of length $2a$, is symmetrically located at a distance $h$ from the top. Over the region of the delamination, the sandwich beam consists of two parts: the delaminated layer of the upper face sheet (referred to as the ''delaminated part,'' of thickness $h$) and the part below the delamination (''substrate part,'' of thickness $f_1-h+c+f_2$, which includes the core and the lower face sheet). The region outside the deamination is referred to as the ''base part'' and consists of the entire section of the sandwich beam, i.e., of thickness $f_1+c+f_2$. We shall also denote the base part with 1, the delaminated part with 2, and the substrate part with 3. Let us also assume that the beam is clamped-clamped.

The characteristic of sandwich construction is that the neutral axis for the base and the substrate parts is in general no longer at the middle of the corresponding sections. With respect to a reference axis $x$ through the middle of the core, the neutral axis of the base section is defined at a distance $e_1$ (Fig. 2), as

$$e_1(E_{f1}f_1+E_cc+E_{f2}f_2)=E_{f2}f_2\left(\frac{f_2}{2}+\frac{c}{2}\right)-E_{f1}f_1\left(\frac{f_1}{2}+\frac{c}{2}\right), \tag{1a}$$

and that of the substrate part is at a distance $e_3$ given by

[1]Presently at Lucent Technologies.

Contributed by the Applied Mechanics Division of THE AMERICAN SOCIETY OF MECHANICAL ENGINEERS for publication in the ASME JOURNAL OF APPLIED MECHANICS. Manuscript received by the ASME Applied Mechanics Division, September 26, 2000; final revision, May 8, 2001. Associate Editor: T. E. Triantafyllijis. Discussion on the paper should be addressed to the Editor, Prof. Robert M. McMeeking, Department of Mechanical and Environmental Engineering University of California–Santa Barbara, Santa Barbara, CA 93106-5070, and will be accepted until four months after final publication of the paper itself in the ASME JOURNAL OF APPLIED MECHANICS.

  

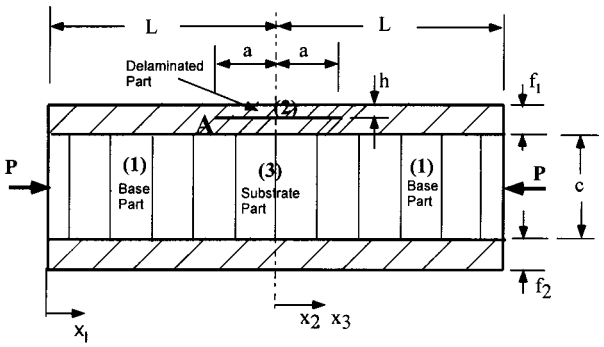


**Fig. 1 Definition of the geometry for a delaminated sandwich beam/plate**

$$e_3[E_{f1}(f_1-h)+E_c c+E_{f2}f_2]=E_{f2}f_2\left(\frac{f_2}{2}+\frac{c}{2}\right)-E_{f1}(f_1-h)\times\left(\frac{f_1-h}{2}+\frac{c}{2}\right). \quad (1b)$$

Moreover, while for the delaminated layer, which is homogeneous, the bending rigidity per unit width is

$$D_2=E_{f1}\frac{h^3}{12}, \quad (2a)$$

for the base part, the equivalent flexural rigidity of the sandwich section per unit width, is (Fig. 2)

$$D_1=E_{f1}\frac{f_1^3}{12}+E_{f1}f_1\left(\frac{f_1}{2}+\frac{c}{2}+e_1\right)^2+E_{f2}\frac{f_2^3}{12}+E_{f2}f_2\times\left(\frac{f_2}{2}+\frac{c}{2}-e_1\right)^2+E_c\frac{c^3}{12}+E_c c e_1^2, \quad (2b)$$

and for the substrate (again, per unit width),

$$D_3=E_{f1}\frac{(f_1-h)^3}{12}+E_{f1}(f_1-h)\left(\frac{f_1-h}{2}+\frac{c}{2}+e_3\right)^2+E_c\frac{c^3}{12}+E_c c e_3^2+E_{f2}\frac{f_2^3}{12}+E_{f2}f_2\left(\frac{f_2}{2}+\frac{c}{2}-e_3\right)^2. \quad (2c)$$

The nonlinear differential equations including transverse shear for the three parts of the sandwich beam-plate (Fig. 1), namely the base part (1), delaminated part (2), and substrate part (3), are (Huang and Kardomateas [15])

$$D_i\frac{d^2\theta}{ds^2}+P\left(\frac{\alpha_i P}{2A_i\bar{G}_i}\sin 2\theta+\sin\theta\right)=0,$$

which, after Taylor series expansion of the sin $\theta$, becomes

$$D_i\frac{d^2\theta_i(x_i)}{dx_i^2}+\left(\frac{\alpha_i P_i^2}{A_i\bar{G}_i}+P_i\right)\theta_i(x_i)-\left(\frac{2\alpha_i P_i^2}{3A_i\bar{G}_i}+\frac{P_i}{6}\right)\theta_i^3(x_i)=0, \quad i=1,2,3 \quad (3a)$$

where $\theta_i(x)$ is the rotation of the normal to the cross section, $D_i$ is the bending rigidity, $\alpha_i$ is the shear correction factor, $P_i$ is the axial load, $A_i$ are the cross-sectional areas and $\bar{G}_i$ is the "average" shear modulus of each part, calculated from the compliances of the constituent phases [15]

$$\frac{f_1+c+f_2}{\bar{G}_1}=\frac{f_1}{G_{f1}}+\frac{c}{G_c}+\frac{f_2}{G_{f2}};\quad \bar{G}_2=G_{f1};$$
$$A_1=(f_1+c+f_2)w;\quad A_2=hw \quad (3b)$$
$$\frac{f_1-h+c+f_2}{\bar{G}_3}=\frac{f_1-h}{G_{f1}}+\frac{c}{G_c}+\frac{f_2}{G_{f2}};$$
$$A_3=(f_1-h+c+f_2)w. \quad (3c)$$

The shear correction factors can be found in Huang and Kardomateas [15]. For the base part (1),

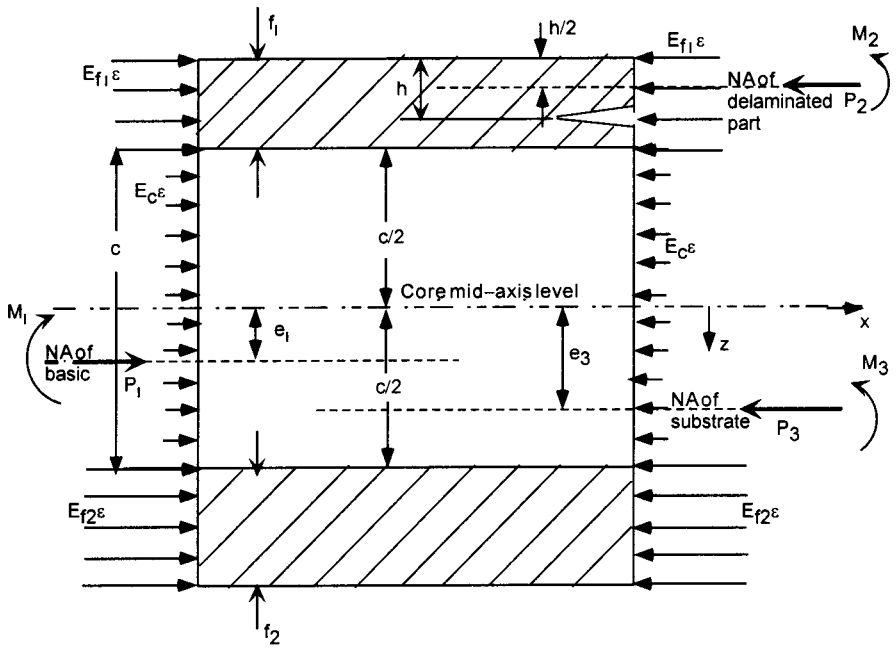


**Fig. 2 Force and moment resultants at the tip of the delamination**

$$\alpha_1=\bar{G}_1A_1w\sum_{i=1,2}\frac{E_{fi}^2}{4D_1^2G_{fi}}\left[a_i^4f_i-\frac{2}{3}a_i^2(a_i^3-b_i^3)+\frac{1}{5}(a_i^5-b_i^5)\right]$$
$$+\frac{E_{fi}^2}{D_1^2G_c}\left[f_i^2c_i^2b_i+\frac{2}{15}\frac{E_c^2}{E_{fi}^2}b_i^5+\frac{2}{3}\frac{E_c}{E_{fi}}f_ic_ib_i^3\right] \quad (3d)$$

where

$$a_i=f_i+\frac{c}{2}+(-1)^{i+1}e_1;\quad b_i=\frac{c}{2}+(-1)^{i+1}e_1;$$
$$c_i=\frac{f_i}{2}+\frac{c}{2}+(-1)^{i+1}e_1,\quad i=1,2. \quad (3e)$$

Notice that since the delaminated part is homogeneous, $\alpha_2=6/5$, and for the substrate part, $\alpha_3$ is found from $(3d,e)$ by substituting $f_1-h$ in place of $f_1$, and $D_3$, $A_3$, $\bar{G}_3$, $e_3$ in place of $D_1$, $A_1$, $\bar{G}_1$, $e_1$.

The way the geometry was configured, gives the following conditions at $x_i=0$:

$$\theta_i(0)=0,\quad i=1,2,3. \quad (4)$$

The above condition is valid for $i=1$ because of the clamped-end and for $i=2,3$ because of symmetry.

Furthermore, a kinematic condition of common slope between the different parts at the section where the delamination starts or ends reads

$$\theta_1(L-a)=\theta_2(-a)=\theta_3(-a)=\theta_A. \quad (5)$$

The force and moment (about the neutral axis of the base part) equilibrium conditions are (Fig. 2)

$$P_1=P_2+P_3, \quad (6)$$

$$M_1-M_2-M_3-P_2\left(f_1+\frac{c}{2}+e_1-\frac{h}{2}\right)+P_3(e_3-e_1)=0. \quad (7)$$

Finally the axial displacement continuity condition at the tip A (Fig. 1) is

$$u_2^A=u_3^A, \quad (8)$$

where

$$u_2^A=\frac{1}{2}\int_{-a}^{0}\theta_2^2dx_2+\frac{P_2a}{E_{f1}wh}+\theta_A\frac{h}{2}, \quad (9)$$

$$u_3^A=\frac{1}{2}\int_{-a}^{0}\theta_3^2dx_3+\frac{P_3a}{[E_{f1}(f_1-h)+E_cc+E_{f2}f_2]w}$$
$$-\theta_A\left(e_3+\frac{c}{2}+f_1-h\right). \quad (10)$$

**Asymptotic Expansion.** Now, let us expand $P_i$ and $\theta_i$ as

$$P_i=P_i^{(0)}+\xi P_i^{(1)}+\xi^2P_i^{(2)}+\xi^3P_i^{(3)}+\ldots, \quad (11)$$

$$\theta_i(x_i)=\xi\theta_i^{(1)}(x_i)+\xi^2\theta_i^{(2)}(x_i)+\xi^3\theta_i^{(3)}(x_i)+\ldots, \quad (12)$$

where the (0) superscript corresponds to the pre-buckling state, the (1) to the buckling state and the (2), etc., to the post-buckling state. Also, let us set $\xi$ to be the common slope of the section at the delamination tip A, i.e.,

$$\xi=\theta_A. \quad (13)$$

From (5) and (12), this gives the additional conditions

$$\theta_1^{(1)}(L-a)=1;\quad \theta_1^{(2)}(L-a)=\theta_1^{(3)}(L-a)=\ldots=0, \quad (14)$$

and

$$\theta_i^{(1)}(-a)=1;\quad \theta_i^{(2)}(-a)=\theta_i^{(3)}(-a)=\ldots=0,\quad i=2,3. \quad (15)$$

Substituting Eqs. (11) and (12) into Eq. (3) and (4)–(10) and rearranging the terms based on the order of $\xi$, we obtain separately the equations and boundary conditions for the pre-buckling, buckling, and initial post-buckling problem. The asymptotic expansion is an efficient way of deriving closed-form solutions for the initial post-buckling behavior and has also been used previously by Kardomateas [5] in the study of delaminations in monolithic composites in conjunction with the elastica theory.

**Pre-buckling State, $O(\xi^0)$.** The major characteristic of the pre-buckling state for a sandwich section is that under uniform compressive strain there are nonzero bending moments (as opposed to a monolithic one in which the bending moments are zero) but zero bending deflections.

Under a uniformly applied compressive strain, $\epsilon_0$, the resultant forces (per unit width) for the base part (1), delaminated part (2), and substrate part (3), are (Fig. 2)

$$P_1^{(0)}=\epsilon_0(E_{f1}f_1+E_cc+E_{f2}f_2), \quad (16a)$$

$$P_2^{(0)}=\epsilon_0E_{f1}h;\quad P_3^{(0)}=\epsilon_0[E_{f1}(f_1-h)+E_cc+E_{f2}f_2]. \quad (16b)$$

The pre-buckling moments (per unit width) are then found as (Fig. 2)

$$M_1^{(0)}=\epsilon_0\left[E_{f1}f_1\left(\frac{f_1}{2}+\frac{c}{2}+e_1\right)+E_cce_1\right.$$
$$\left.-E_{f2}f_2\left(\frac{f_2}{2}+\frac{c}{2}-e_1\right)\right];\quad M_2^{(0)}=0, \quad (17a)$$

$$M_3^{(0)}=\epsilon_0\left[E_{f1}(f_1-h)\left(\frac{f_1-h}{2}+\frac{c}{2}+e_3\right)+E_cce_3\right.$$
$$\left.-E_{f2}f_2\left(\frac{f_2}{2}+\frac{c}{2}-e_3\right)\right]. \quad (17b)$$

These pre-buckling forces and moments satisfy identically the force and moment equilibrium equation (about the neutral axis of the base part), Eqs. (6) and (7). Furthermore, since a state of pure axial compressive strain exists without bending deflections, the compatibility of shortening, Eq. (8) is also satisfied.

**Buckling (First-Order) Equations, $O(\xi^1)$.** From (3) and (11,12), the first-order differential equation for the three parts is

$$D_i\frac{d^2\theta_i^{(1)}(x_i)}{dx_i^2}+\left(\frac{\alpha_iP_i^{(0)2}}{A_i\bar{G}_i}+P_i^{(0)}\right)\theta_i^{(1)}(x_i)=0,\quad i=1,2,3 \quad (18a)$$

and the corresponding boundary conditions from (4) are

$$\theta_i^{(1)}(0)=0,\quad i=1,2,3, \quad (18b)$$

and from (5),

$$\theta_1^{(1)}(L-a)=\theta_2^{(1)}(-a)=\theta_3^{(1)}(-a)=\theta_A^{(1)}=1. \quad (18c)$$

The first-order moment equilibrium from (7) is

$$D_1\frac{d\theta_1^{(1)}}{dx_1}\bigg|_{x_1=L-a}-D_2\frac{d\theta_2^{(1)}}{dx_2}\bigg|_{x_2=-a}-D_3\frac{d\theta_3^{(1)}}{dx_3}\bigg|_{x_3=-a}$$
$$-P_2^{(1)}\left(f_1+\frac{c}{2}+e_1-\frac{h}{2}\right)+P_3^{(1)}(e_3-e_1)=0, \quad (18d)$$

and the first-order force equilibrium,

$$P_2^{(1)}+P_3^{(1)}=P_1^{(1)}. \quad (18e)$$

Finally, the first-order compatibility equation from (8) becomes, since $\theta_A^{(1)}=1$,

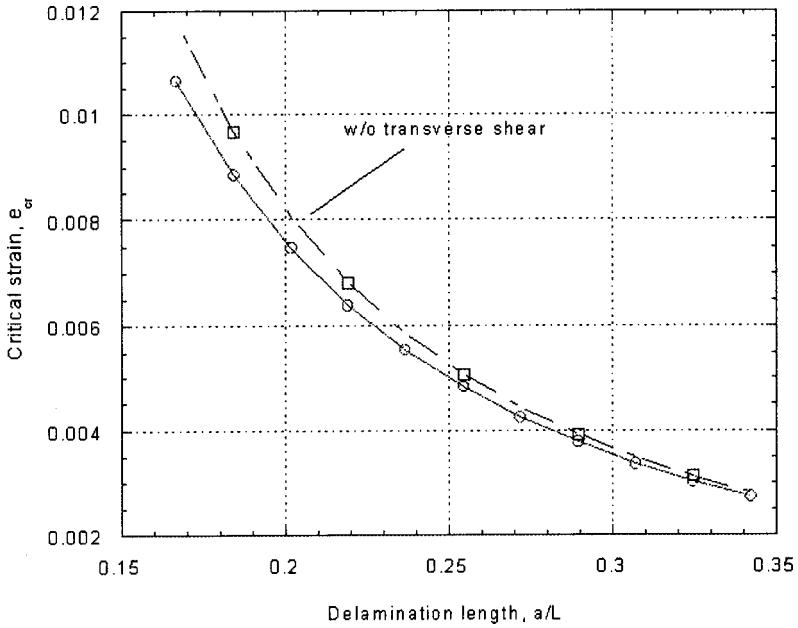


**Fig. 3 Critical strain versus delamination length for the case of a glass-polyester/PVC sandwich composite**

$$\frac{P_3^{(1)}a}{[E_{f1}(f_1-h)+E_c c+E_{f2}f_2]w}-\left(e_3+\frac{c}{2}+f_1-h\right)=\frac{P_2^{(1)}a}{E_{f1}hw}+\frac{h}{2}. \tag{18g}$$

Let's set

$$\lambda_i=\sqrt{\left(\frac{\alpha_i P_i^{(0)2}}{A_i\bar{G}_i}+P_i^{(0)}\right)\Big/ D_i},\quad i=1,2,3 \tag{19}$$

where $P_1^{(0)}$, $P_2^{(0)}$, and $P_3^{(0)}$ are given in (16) in terms of the uniform compressive strain $\epsilon_0$. Then, the solutions for Eqs. (18*a*) that satisfies the boundary conditions (18*b*), is

$$\theta_i^{(1)}=C_i^{(1)}\sin(\lambda_i x_i),\quad i=1,2,3. \tag{20}$$

Now, the constants $C_1^{(1)}$, $C_2^{(1)}$, $C_3^{(1)}$ are determined from the common slope Eq. (18*c*), as

$$C_1^{(1)}=1/\sin\lambda_1(L-a);\quad C_2^{(1)}=-1/\sin\lambda_2 a;\quad C_3^{(1)}=-1/\sin\lambda_3 a. \tag{21}$$

The characteristic equation is found in terms of $\epsilon_0$ by eliminating $P_1^{(1)}$, $P_2^{(1)}$, and $P_3^{(1)}$ from the previous equations. This is done as follows.

The moment equilibrium Eq. (18*d*), becomes

$$D_1\lambda_1\cot\lambda_1(L-a)+D_2\lambda_2\cot\lambda_2 a+D_3\lambda_3\cot\lambda_3 a =P_2^{(1)}\left(f_1+\frac{c}{2}+e_1-\frac{h}{2}\right)-P_3^{(1)}(e_3-e_1). \tag{22a}$$

By using the neutral axis definitions (1*a*) and (1*b*), we obtain

$$e_3-e_1=\left(f_1+\frac{c}{2}+e_1-\frac{h}{2}\right)\frac{E_{f1}h}{[E_{f1}(f_1-h)+E_c c+E_{f2}f_2]}, \tag{22b}$$

therefore (22*a*) becomes

$$P_2^{(1)}\frac{a}{E_{f1}hw}-P_3^{(1)}\frac{a}{[E_{f1}(f_1-h)+E_c c+E_{f2}f_2]w} =\frac{[D_1\lambda_1\cot\lambda_1(L-a)+D_2\lambda_2\cot\lambda_2 a+D_3\lambda_3\cot\lambda_3 a]a}{E_{f1}hw\left(f_1+\frac{c}{2}+e_1-\frac{h}{2}\right)}. \tag{23}$$

By comparing (18*g*) and (23), we can see that the left-hand side of (23) can be eliminated. Thus, we obtain the following characteristic equation:

$$\frac{[D_1\lambda_1\cot\lambda_1(L-a)+D_2\lambda_2\cot\lambda_2 a+D_3\lambda_3\cot\lambda_3 a]a}{E_{f1}hw\left(f_1+\frac{c}{2}+e_1-\frac{h}{2}\right)} +\left(e_3+\frac{c}{2}+f_1-\frac{h}{2}\right)=0. \tag{24}$$

Equation (24) is a nonlinear algebraic equation which can be solved numerically for the critical strain $\epsilon_0$ (or critical load from (16)). In the numerical procedure, a solution is sought near the Euler buckling strain of the delaminated layer, which is $\epsilon_0=\pi^2h^2/(12a^2)$.

**Initial Post-buckling, Second-order Equations, $O(\xi^2)$.** From (3) and (11,12), we obtain the second-order differential equation

$$D_i\frac{d^2\theta_i^{(2)}(x_i)}{dx_i^2}+\left(\frac{\alpha_i P_i^{(0)2}}{A_i\bar{G}_i}+P_i^{(0)}\right)\theta_i^{(2)}(x_i) =-\left(\frac{2\alpha_i P_i^{(0)}P_i^{(1)}}{A_i\bar{G}_i}+P_i^{(1)}\right)\theta_i^{(1)}(x_i),\quad i=1,2,3 \tag{25}$$

and from (4) and (14,15),

$$\theta_i^{(2)}(0)=0,\quad i=1,2,3 \tag{26a}$$

$$\theta_1^{(2)}(L-a)=\theta_2^{(2)}(-a)=\theta_3^{(2)}(-a)=0. \tag{26b}$$

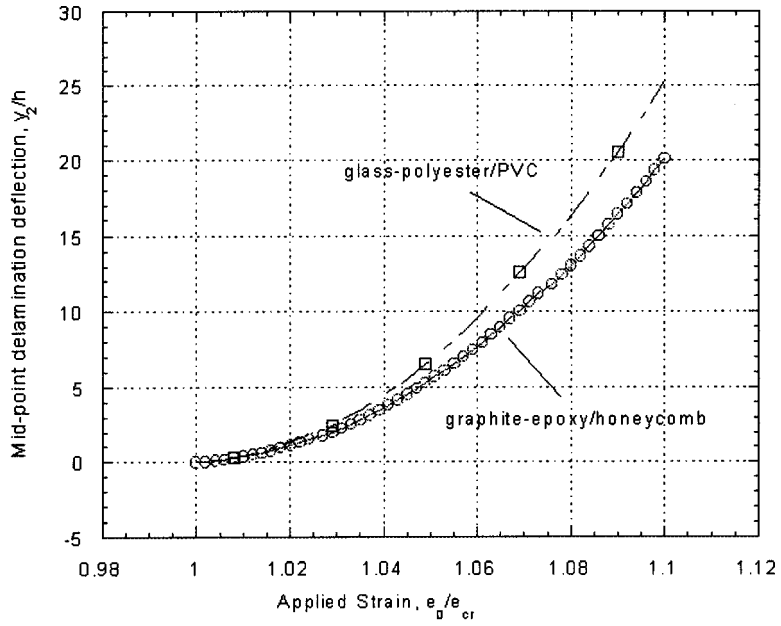


(*a*)

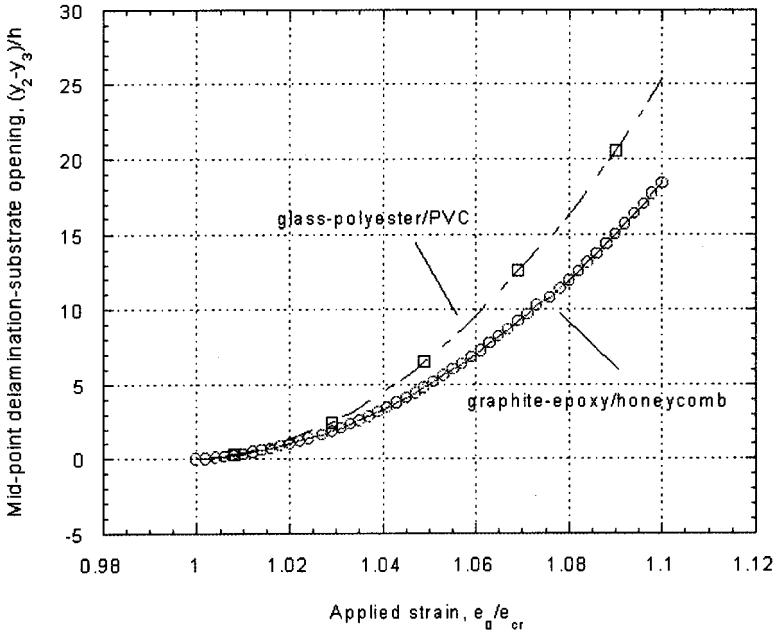


(*b*)

**Fig. 4 (*a*) Comparison of the two material sandwich systems with regard to the delamination midpoint deflection during the initial post-buckling phase. (*b*) Comparison of the two material sandwich systems with regard to the midpoint delamination-substrate opening during the initial post-buckling phase.**

The second-order moment equilibrium from (7) is

$$D_1\frac{d\theta_1^{(2)}}{dx_1}\bigg|_{x_1=L-a}-D_2\frac{d\theta_2^{(2)}}{dx_2}\bigg|_{x_2=-a}-D_3\frac{d\theta_3^{(2)}}{dx_3}\bigg|_{x_3=-a}$$
$$-P_2^{(2)}\left(f_1+\frac{c}{2}+e_1-\frac{h}{2}\right)+P_3^{(2)}(e_3-e_1)=0, \qquad (27)$$

and the second-order force equilibrium is

$$P_2^{(2)}+P_3^{(2)}=P_1^{(2)}. \qquad (28)$$

Finally, the second-order displacement compatibility from (8)–(10) and (11,12) is

$$\frac{1}{2}\int_{-a}^{0}\theta_3^{(1)^2}(x_3)dx_3+\frac{P_3^{(2)}a}{w[E_{f1}(f_1-h)+E_cc+E_{f2}f_2]}$$
$$=\frac{1}{2}\int_{-a}^{0}\theta_2^{(1)^2}(x_2)dx_2+\frac{P_2^{(2)}a}{E_{f1}wh}. \qquad (29)$$

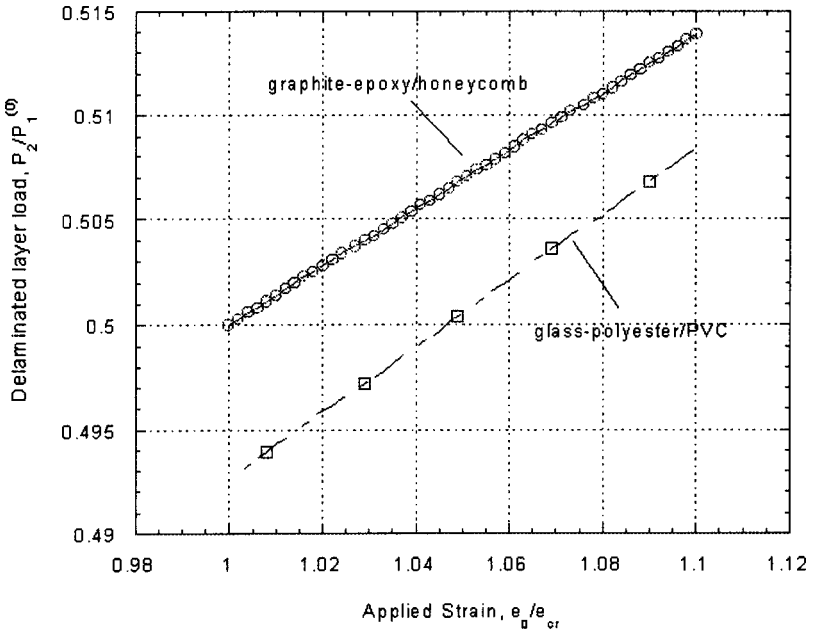


(*a*)

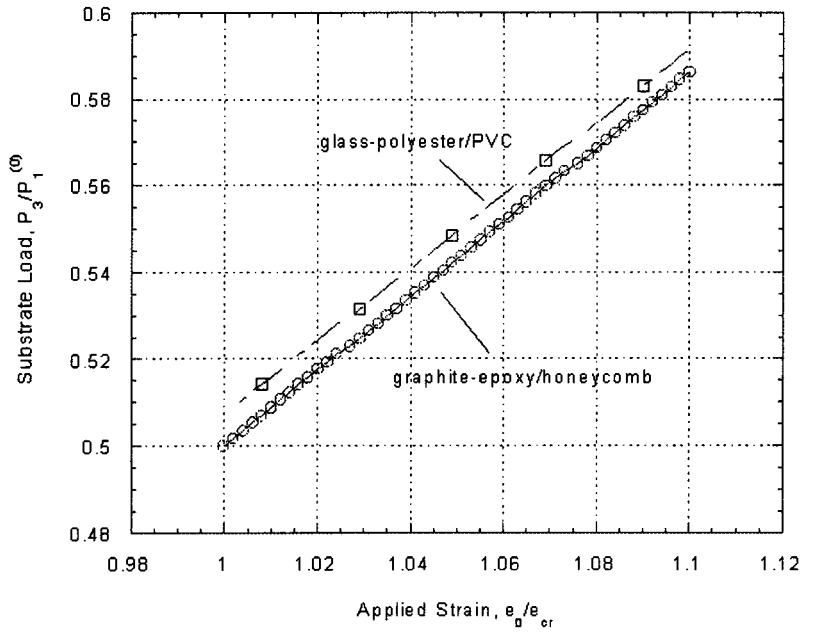


(*b*)

**Fig. 5 (*a*) Comparison of the two material sandwich systems with regard to the delamination load during the initial post-buckling phase. (*b*) Comparison of the two material sandwich systems with regard to the substrate load during the initial post-buckling phase.**

The general solution for the second-order differential Eq. (25) is

$$\theta_i^{(2)}(x_i) = C_i^{(2)} \sin \lambda_i x_i + B_i^{(2)} \cos \lambda_i x_i + \frac{P_i^{(1)}}{2\lambda_i D_i}\left(\frac{2\alpha_i P_i^{(0)}}{A_i \bar{G}_i} + 1\right) C_i^{(1)} x_i \cos \lambda_i x_i . \quad (30)$$

The constants $B_i^{(2)}$ are zeros due to the boundary conditions (26*a*),

$$B_i^{(2)} = 0, \quad i = 1,2,3. \quad (31)$$

Applying the conditions (26*b*), we can find the constants $C_i^{(2)}$ as

$$C_1^{(2)} = -\frac{P_1^{(1)}}{2\lambda_1 D_1} C_1^{(1)} (L-a) \cot \lambda_1 (L-a)\left(\frac{2\alpha_1 P_1^{(0)}}{A_1 \bar{G}_1} + 1\right), \quad (32a)$$

and

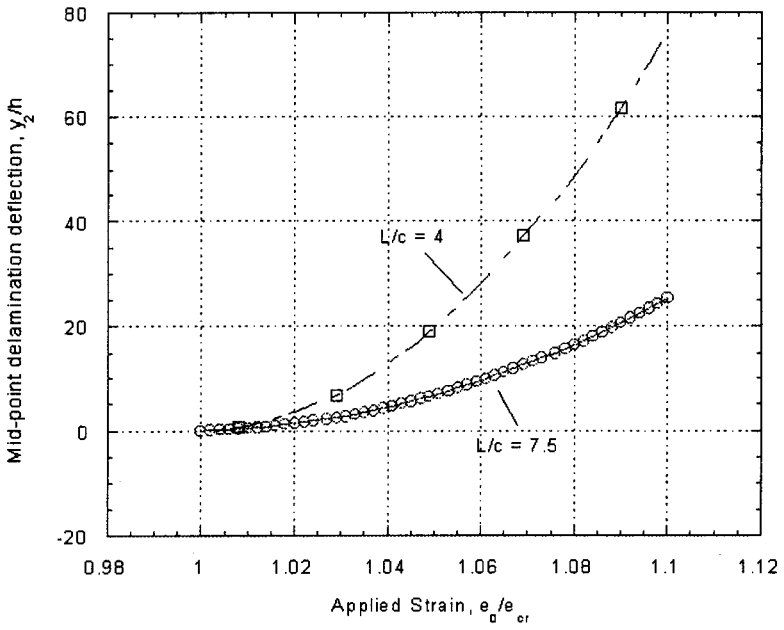


**Fig. 6 Effect of the length over core thickness aspect ratio on the midpoint delamination deflection during the initial post-buckling phase for glass-epoxy/polyester**

$$C_i^{(2)} = -\frac{P_i^{(1)}}{2\lambda_i D_i} C_i^{(1)} a \cot \lambda_i a \left( \frac{2\alpha_i P_i^{(0)}}{A_i \bar{G}_i} + 1 \right), \quad i = 2,3. \tag{32b}$$

Now the displacement compatibility Eq. (29), becomes

$$P_2^{(2)} \frac{a}{E_{f1} wh} - P_3^{(2)} \frac{a}{w[E_{f1}(f_1 - h) + E_c c + E_{f2} f_2]} = \frac{1}{4}\left[ C_3^{(1)2}\left( a - \frac{\sin 2\lambda_3 a}{2\lambda_3} \right) - C_2^{(1)2}\left( a - \frac{\sin 2\lambda_2 a}{2\lambda_2} \right) \right]. \tag{33}$$

The moment equilibrium (27), by substituting the second-order deflections (30) and again the relationship for the neutral axes of the substrate and the base part (22*b*), becomes

$$\left[ P_2^{(2)} \frac{a}{E_{f1} wh} - P_3^{(2)} \frac{a}{w[E_{f1}(f_1 - h) + E_c c + E_{f2} f_2]} \right] \times \frac{E_{f1} wh \left( f_1 + \frac{c}{2} + e_1 - \frac{h}{2} \right)}{a} = D_1 \left\{ C_1^{(2)} \lambda_1 \cos \lambda_1 (L-a) + \frac{C_1^{(1)} P_1^{(1)}}{2\lambda_1 D_1} \left( \frac{2\alpha_1 P_1^{(0)}}{A_1 \bar{G}_1} + 1 \right) \times [\cos \lambda_1 (L-a) - (L-a)\lambda_1 \sin \lambda_1 (L-a)] \right\} - \sum_{i=2,3} D_i \left[ C_i^{(2)} \lambda_i \cos \lambda_i a + \frac{C_i^{(1)} P_i^{(1)}}{2\lambda_i D_i} \left( \frac{2\alpha_i P_i^{(0)}}{A_i \bar{G}_i} + 1 \right) \times (\cos \lambda_i a - a\lambda_i \sin \lambda_i a) \right]. \tag{34}$$

Comparing (34) and (33), we can eliminate the left-hand side of the latter equation, which contains the second-order forces, and, by using also (32), thus obtain one equation for the first-order forces, i.e.,

$$a_2 P_2^{(1)} + a_3 P_3^{(1)} = \frac{1}{4}\left[ C_3^{(1)2}\left( a - \frac{\sin 2\lambda_3 a}{2\lambda_3} \right) - C_2^{(1)2} \times \left( a - \frac{\sin 2\lambda_2 a}{2\lambda_2} \right) \right] \frac{E_{f1} wh \left( f_1 + \frac{c}{2} + e_1 - \frac{h}{2} \right)}{a}, \tag{35}$$

where

$$a_i = \frac{C_1^{(1)}}{2\lambda_1} \left( \frac{2\alpha_1 P_1^{(0)}}{A_1 \bar{G}_1} + 1 \right) \left[ \cos \lambda_1 (L-a) - \frac{(L-a)\lambda_1}{\sin \lambda_1 (L-a)} \right] + \frac{C_i^{(1)}}{2\lambda_i} \left( \frac{2\alpha_i P_i^{(0)}}{A_i \bar{G}_i} + 1 \right) \left( \frac{a\lambda_i}{\sin \lambda_i a} - \cos \lambda_i a \right), \quad i = 2,3.$$

The second equation for the first-order forces is the first-order compatibility Eq. (18*g*).

The system of these two linear equations, (35) and (18*g*), can be solved for the first-order forces, $P_2^{(1)}$ and $P_3^{(1)}$.

The solution for the higher-order terms can proceed in the same fashion.

The first-order applied load $P_1^{(1)}$ is in turn found from the second-order force equilibrium, Eq. (28). Notice that from (11), since $P_1^{(0)} = P_{cr}$, the perturbation parameter $\xi$ can be found from the applied external load, $\bar{P}$, as

$$\xi = \frac{\bar{P} - P_{cr}}{P_1^{(1)}}. \tag{36}$$

This, of course, presumes that we only account for the first-order load terms.

**Deflections.** The deflections can be found by integrating the relationship (Huang and Kardomateas [15])

$$\frac{dy_i}{dx_i}=\sin\theta_i+\frac{\alpha_i P_i}{2A_i\overline{G}_i}\sin 2\theta_i\,. \tag{37a}$$

Introducing the asymptotic expansions (11) and (12) and the first and second-order expressions (20) and (30), gives

$$\frac{dy_i}{dx_i}=\xi\left(1+\frac{\alpha_i P_i^{(0)}}{\overline{G}_i A_i}\right)\theta_i^{(1)}+\xi^2\left[\left(1+\frac{\alpha_i P_i^{(0)}}{\overline{G}_i A_i}\right)\theta_i^{(2)}+\frac{\alpha_i P_i^{(1)}}{\overline{G}_i A_i}\theta_i^{(1)}\right]+O(\xi^3), \tag{37b}$$

and therefore by integrating with the boundary condition

$$y_1(0)=0;\quad \text{and } y_i(-a)=0;\quad i=2,3 \tag{37c}$$

gives the first-order deflections as

$$y_1^{(1)}=\frac{C_1^{(1)}}{\lambda_1}\left(1+\frac{\alpha_1 P_1^{(0)}}{\overline{G}_1 A_1}\right)(1-\cos\lambda_1 x_1), \tag{38a}$$

$$y_i^{(1)}=\frac{C_i^{(i)}}{\lambda_i}\left(1+\frac{\alpha_i P_i^{(0)}}{\overline{G}_i A_i}\right)(\cos\lambda_i a-\cos\lambda_i x_i);\quad i=2,3 \tag{38b}$$

and the second-order deflections as

$$y_1^{(2)}=\left(1+\frac{\alpha_1 P_1^{(0)}}{\overline{G}_1 A_1}\right)\left[\left(\frac{Q_1^{(1)}}{\lambda_1^2}-\frac{C_1^{(2)}}{\lambda_1}\right)(\cos\lambda_1 x_1-1)+\frac{Q_1^{(1)}}{\lambda_1}x_1\sin\lambda_1 x_1\right]+\frac{C_1^{(1)}}{\lambda_1}\frac{\alpha_1 P_1^{(1)}}{\overline{G}_1 A_1}(1-\cos\lambda_1 x_1), \tag{39a}$$

$$y_i^{(2)}=\left(1+\frac{\alpha_i P_i^{(0)}}{\overline{G}_i A_i}\right)\left[\left(\frac{Q_i^{(1)}}{\lambda_i^2}-\frac{C_i^{(2)}}{\lambda_i}\right)(\cos\lambda_i x_i-\cos\lambda_i a)+\frac{Q_i^{(1)}}{\lambda_i}(x_i\sin\lambda_i x_i-a\sin\lambda_i a)\right]+\frac{C_i^{(1)}}{\lambda_i}\frac{\alpha_i P_i^{(1)}}{\overline{G}_i A_i}(\cos\lambda_i a-\cos\lambda_i x_i);\quad i=2,3 \tag{39b}$$

where

$$Q_i^{(1)}=\frac{P_i^{(1)}C_i^{(1)}}{2\lambda_i D_i}\left(\frac{2\alpha_i P_i^{(0)}}{\overline{G}_i A_i}+1\right);\quad i=1,2,3. \tag{39c}$$

## Discussion of Results

For an illustration of the results from the previous analysis, consider a sandwich beam with (in mm) $f_1=f_2=3$, $c=25$, $h=3$, $w=20$, and $L=150$. Two types of core were used: (a) a PVC core with (in MPa) $E_c=93$, $G_c=35$, and (b) an aluminum honeycomb core with $E_c=1$, $G_c=200$ (data from Gibson and Asby [16]). The corresponding face-sheets were (a) E-glass/polyester unidirectional with (in GPa) $E_{f1}=E_{f2}=26$ and $G_{f1}=G_{f2}=3$ and (b) graphite/epoxy unidirectional with $E_{f1}=E_{f2}=140$ and $G_{f1}=G_{f2}=5$. In the results presented, the case of no transverse shear effect corresponds to $\alpha_i=0$.

The shear correction factors for the case of glass-polyester/PVC system are $\alpha_1=1.215$, $\alpha_2=1.200$, and $\alpha_3=1.044$. More important are the corresponding ratios $\alpha_i/\overline{G}_i A_i$, as these represent the magnitude of the effect of transverse shear and these were, respectively, $0.453\times10^{-4}$, $0.667\times10^{-5}$, and $0.476\times10^{-4}$. The first and the last numbers are larger because they include the core, unlike the second number which is for the delaminated layer only. For the graphite-epoxy/honeycomb, the corresponding data are $\alpha_1=1.209$, $\alpha_2=1.200$, and $\alpha_3=0.482$, whereas the $\alpha_i/\overline{G}_i A_i$ ratios are $0.794\times10^{-5}$, $0.400\times10^{-5}$, and $0.386\times10^{-5}$. The last set of numbers shows the importance of the low extensional modulus of the honeycomb core.

Figure 3 shows the critical strain, $\epsilon_{cr}$ for a range of delamination lengths in the case of sandwich material system (a). It is seen that the critical strain decreases with longer delaminations, as expected, and that the effect of transverse shear is to lower the critical strain, again as expected.

The initial post-buckling results which follow are produced for delamination length $a=L/3$. This solution is an asymptotic solution, so accuracy is expected to be compromised as we move away from the critical point. Figure 4($a$) shows the midpoint delamination deflection versus applied strain for the two material systems and Fig. 4($b$) shows the midpoint delamination-substrate opening. Both deflections are higher for the glass-polyester/PVC case, which is expected due to the lower stiffness of the face sheet. The delamination load (normalized with the critical load) is shown in Fig. 5($a$) and the substrate load is shown in Fig. 5($b$). For both material systems the delamination load and the substrate load increases with applied strain, but no definite trend exists between the two material systems—the normalized (with $P_{cr}$) delamination load being higher in the material system (b) but the normalized substrate load being higher in the material system (a).

Finally, Fig. 6 shows the effect of the length over core thickness aspect ratio on the midpoint delamination deflection during the initial post-buckling phase for glass-epoxy/polyester material system. The face sheet thickness and delamination length was kept constant and the critical strain is essentially the same in both cases (slightly lower for the higher aspect ratio). But the case of a thicker core (lower aspect ratio) shows a higher delamination deflection.

## Acknowledgments

The financial support of the Office of Naval Research, Ship Structures S & T Division, Grant N00014-90-J-1995, and of the Air Force Office of Scientific Research, Grant F49620-98-1-0384, and the interest and encouragement of the Grant Monitors, Dr. Y. D. S. Rajapakse, Dr. Brian Sanders, and Dr. Ozden Ochoa are both gratefully acknowledged. The authors would also like to acknowledge valuable discussions regarding sandwich material properties with Prof. Leif Carlsson, Florida Atlantic University.

## References

[1] Yin, W. L., Sallam, S., and Simitses, G. J., 1986, "Ultimate Axial Load Capacity of a Delaminated Beam-Plate," AIAA J., **24**(1), pp. 123–128.
[2] Simitses, G. J., Sallam, S., and Yin, W. L., 1985, "Effect of Delamination on Axially Loaded Homogeneous Laminated Plates," AIAA J., **23**, pp. 1437–1444.
[3] Chai, H., Babcock, C. D., and Knauss, W. G., 1981, "One Dimensional Modeling of Failure in Laminated Plates by Delamination Buckling," Int. J. Solids Struct., **17**(11), pp. 1069–1083.
[4] Whitcomb, J. D., 1981, "Finite Element Analysis of Instability-Related Delamination Growth," NASA TM 81964, Mar.
[5] Shivakumar, K. N., and Whitcomb, J. D., 1985, "Buckling of a Sublaminate in a Quasi-Isotropic Composite Laminate," J. Compos. Mater., **19**, Jan., pp. 2–18.
[6] Kardomateas, G. A., 1990, "Postbuckling Characteristics in Delaminated Kevlar/Epoxy Laminates: An Experimental Study," J. Compos. Technol. Res., **12**(2), pp. 85–90.
[7] Kardomateas, G. A., 1993, "The Initial Postbuckling and Growth Behavior of Internal Delaminations in Composite Plates," ASME J. Appl. Mech., **60**, pp. 903–910.
[8] Kardomateas, G. A., Pelegri, A. A., and Malik, B., 1995, "Growth of Internal Delaminations Under Cyclic Compression in Composite Plates," J. Mech. Phys. Solids, **43**(6), pp. 847–868.
[9] Kant, T., and Patil, H. S., 1991, "Buckling Load of Sandwich Columns With a Higher-Order Theory," J. Reinf. Plast. Compos., **10**(1), pp. 102–109.

[10] Hunt, G. E., and Da Silva, L. S., 1990, ''Interaction Bending Behavior of Sandwich Beams,'' ASME J. Appl. Mech., **57**, pp. 189–196.
[11] Hunt, G. E., and Da Silva, L. S., 1990, ''Interactive Buckling in Sandwich Structures With Core Orthotropy,'' Int. J. Mech. Struct. Mech., **18**(3), pp. 353–372.
[12] Frostig, Y., 1992, ''Behavior of Delaminated Sandwich Beams With Transversely Flexible Core—High Order Theory,'' Composite Structures, **20**, pp. 1–16.
[13] Frostig, Y., and Baruch, M., 1993, ''Buckling of Simply-Supported Sandwich Beams With Transversely Flexible Core—A High Order Theory,'' J. Eng. Mech. Div., **119**(5), pp. 955–972.
[14] Rajapakse Y. D. S., Kardomateas G. A., and Birman V., eds, 2000, *Mechanics of Sandwich Structures*, AD-Vol. 62/AMD-Vol. 245, ASME, New York.
[15] Huang, H., and Kardomateas, G. A., 2002, ''Buckling and Postbuckling of Sandwich Beams Including Transverse Shear,'' AIAA J., **40**(11), pp. 2331–2335.
[16] Gibson, L. J., and Ashby, M. F., 1997, *Cellular Solids—Structure and Properties*, 2nd Ed., Cambridge University Press, Cambridge, UK.